Collision of domain walls and reheating of the brane universe

Yu-ichi Takamizu[1,*] and Kei-ichi Maeda[1,2,3,†]

[1]*Department of Physics, Waseda University, Okubo 3-4-1, Shinjuku, Tokyo 169-8555, Japan*
[2]*Advanced Research Institute for Science and Engineering, Waseda University, Okubo 3-4-1, Shinjuku, Tokyo 169-8555, Japan*
[3]*Waseda Institute for Astrophysics, Waseda University, Okubo 3-4-1, Shinjuku, Tokyo 169-8555, Japan*

(Received 24 June 2004; published 9 December 2004)

We study particle production at the collision of two domain walls in 5-dimensional Minkowski spacetime. This may provide the reheating mechanism of an ekpyrotic (or cyclic) brane universe, in which two BPS branes collide and evolve into a hot big bang universe. We evaluate a production rate of particles confined to the domain wall. The energy density of created particles is given as $\rho \approx 20\bar{g}^4 N_b m_\eta^4$ where $\bar{g}$ is a coupling constant of particles to a domain-wall scalar field, N_b is the number of bounces at the collision and m_η is the fundamental mass scale of the domain wall. It does not depend on the width d of the domain wall, although the typical energy scale of created particles is given by $\omega \sim 1/d$. The reheating temperature is evaluated as $T_R \approx 0.88\bar{g}N_b^{1/4}$. In order to have the baryogenesis at the electro-weak energy scale, the fundamental mass scale is constrained as $m_\eta \gtrsim 1.1 \times 10^7$ GeV for $\bar{g} \sim 10^{-5}$.

DOI: 10.1103/PhysRevD.70.123514 PACS numbers: 98.80.Cq

I. INTRODUCTION

The big bang theory is very successful because it naturally explains the evolution of our universe from nucleosynthesis to the present time with many observational data. However, it contains some key theoretical problems such as the flatness and the horizon problems [1,2]. So far, only the idea of inflation provides a resolution of those problems. Not only does it give some picture of the earlier stage of the universe before the big bang but also it seems to be supported by some recent observational data on the cosmic microwave background (CMB). While, it is still unclear what the origin of inflaton is. So far, there is no convincing link with fundamental unified theories such as string/M theory.

Recently a new paradigm on the early universe has been proposed, the so-called brane world [3,4]. Such speculation has been inspired by recent developments in string/M theory [5–7]. There has been tremendous work on this scheme of dimensional reduction, where ordinary matter fields are confined to a lower-dimensional hypersurface, while only gravitational fields propagate throughout all of spacetime. In particular, it has been shown that the 10-dimensional $E_8 \times E_8$ heterotic string theory, which is a strong candidate to describe our real world, is equivalent to an 11-dimensional M theory compactified to $\mathbf{M}^{10} \times \mathbf{S}^1/Z_2$ [5]. Furthermore 10-dimensional spacetime is expected to be compactified into $\mathbf{M}^4 \times \mathbf{CY}^6$, where $\mathbf{M}^4$ and $\mathbf{CY}^6$ are 4-dimensional Minkowski spacetime and 6-dimensional Calabi-Yau space, respectively. Randall and Sundrum [8] also proposed a new model where four-dimensional Newtonian gravity is recovered at low energies even without compact extra dimensions. Based on such a new world picture, many cosmological scenarios have been studied [9–11]. See also recent reviews [12–15]. We have found some deviations from standard cosmology by modifications of 4-dimensional Einstein equations on the brane [16], even for the case there is a scalar field in bulk [17].

In such a brane world scenario, for resolving the above-mentioned key theoretical problems in the big bang theory, a new idea of the early universe has been proposed, which is called the ekpyrotic scenario or the cyclic universe scenario [18,19]. It is based on a collision of two cold branes. The universe starts with a cold, empty, and nearly BPS ground state, which contains two parallel branes at rest. The two branes approach each other and then collide. The energy is dissipated on the brane and the big bang universe starts. The BPS state is required in order to retain a supersymmetry in a low-energy 4-dimensional effective action. The visible and hidden branes are flat and are described by a Minkowski spacetime, but the bulk is warped along the fifth dimension. Since this scenario is not only motivated by the fundamental unified theory but also may resolve the key theoretical problems, such as the flatness and horizon problems, it would be very attractive. There has been much discussion about density perturbations to see whether this scenario is really a reliable scenario for the early universe [20–23].

On the other hand, even though there are some works by [24,25], the reheating process itself in this scenario has not been so far investigated in detail. Hence, in this paper, we study how we can recover the hot big bang universe after the collision of the branes. Here we investigate quantum creation of particles, which are confined to the brane, at the collision of two branes. It may be difficult to deal properly with the collision of two branes in basic string theory. Hence, in this paper, we adopt a domain wall constructed by some scalar field as a brane, and analyze the collision of two domain walls in a 5-

*Electronic address: takamizu@gravity.phys.waseda.ac.jp
†Electronic address: maeda@gravity.phys.waseda.ac.jp

dimensional bulk spacetime. Some other studies have also adopted such a picture [26,27]. It is worth noting that there is a thick domain-wall model for a brane world [28].

In order to analyze particle creation at the brane collision, in this paper we consider the simplest situation. We discuss the collision of two domain walls collide in 5D Minkowski spacetime. In Sec. II, we analyze the collision of two domain walls. Then, in Sec. III, we investigate particle creation on the wall at the collision. Applying the particle production to the energy dissipation of the brane, we discuss the reheating mechanism of a brane universe. We use the unit of $c = \hbar = 1$.

II. COLLISION OF TWO DOMAIN WALLS

A. Basic Equations and Initial Setting

We study the collision of two flat domain walls in 5-dimensional (5D) Minkowski spacetime. To construct a domain-wall structure, we adopt a real scalar field Φ with a double-well potential,

$$V(\Phi) = \frac{\lambda}{4}(\Phi^2 - \eta^2)^2, \tag{2.1}$$

where the potential minima are located at $\Phi = \pm\eta$.

Since we discuss the collision of two parallel domain walls, the scalar field is assumed to depend only on a time coordinate t and one spatial coordinate y. The remaining three spatial coordinates are denoted by $\boldsymbol{x}$. For numerical analysis, we use dimensionless parameters and variables, which are rescaled by η (or its mass scale $m_\eta = \eta^{2/3}$) as

$$\tilde{t} = m_\eta t, \quad \tilde{y} = m_\eta y, \quad \tilde{\Phi} = \frac{\Phi}{\eta}, \quad \tilde{\lambda} = m_\eta \lambda. \tag{2.2}$$

In what follows, we omit the tilde in dimensionless variables for brevity.

The equation of motion for Φ in 5D is given by

$$\ddot{\Phi} - \Phi'' + \lambda\Phi(\Phi^2 - 1) = 0, \tag{2.3}$$

where $\dot{}$ and $'$ denote $\partial/\partial t$ and $\partial/\partial y$, respectively.

Equation (2.3) has a static kink solution (K), which is topologically stable. It is called a domain wall, which is described by

$$\Phi_K(y) = \tanh\left[\frac{y}{d}\right], \tag{2.4}$$

where $d = \sqrt{2/\lambda}$ is the thickness of the wall [29]. We also find another stable solution, that is, the antikink solution ($\bar{K}$), which is obtained from Eq. (2.4) by reflecting the spatial coordinate y as $\Phi_{\bar{K}}(y) = \Phi_K(-y) = -\Phi_K(y)$. When a domain wall moves with constant speed v in the y direction, we obtain correspoding solution by boosting Eq. (2.4) as

$$\Phi_v(y, t) = \tanh\left[\frac{\gamma}{d}(y - vt)\right], \tag{2.5}$$

where we assume that the domain wall is initially located at $y = 0$, and $\gamma = 1/\sqrt{1 - v^2}$ is the Lorentz factor.

In order to discuss the collision of two domain walls, we first have to set up the initial data. Using Eq. (2.5), we can construct such an initial data as follows. Provide a kink solution at $y = -y_0$ and an antikink solution at $y = y_0$, which are separated by a large distance and approaching each other with the same speed v. We then obtain the following explicit profile;

$$\Phi(y, 0) = \Phi_v(y + y_0, 0) - \Phi_{-v}(y - y_0, 0) - 1. \tag{2.6}$$

The initial value of $\dot{\Phi}$ is also given by

$$\dot{\Phi}(y, 0) = \dot{\Phi}_v(y + y_0, 0) - \dot{\Phi}_{-v}(y - y_0, 0). \tag{2.7}$$

The spatial separation between two walls is given by $2y_0$, and as long as the separation distance is much larger than the thickness of the wall ($y_0 \gg d$), the initial conditions (2.6) and (2.7) give a good approximation for two moving domain walls. Using these initial values, we solve the dynamical Eq. (2.3) numerically, whose results will be shown in the next subsection.

B. Time Evolution of Domain Walls

We use a numerical approach to solve the equations for the colliding domain walls. The numerical method is shown in Appendix A. We have two free parameters in our simulation of the two-wall collision, i.e., a wall thickness $d = \sqrt{2/\lambda}$ and an initial wall velocity v. The collision of two walls has been discussed in 4-dimensional Minkowski space [30]. Although we discuss the domain-wall collision in 5-dimensional Minkowski space, our basic equations are exactly the same as the cited case, and we find the same results as there. In particular, the results are very sensitive to the initial velocity v.

First let us show the numerical results for two typical initial velocities, i.e., $v = 0.2$ and 0.4, in Figs. 1–4. The evolution of Φ is depicted in Figs. 1 and 3, while that of the energy density is shown in Figs. 2 and 4. The energy density of the scalar field is given by

$$\rho_\Phi = \frac{1}{2}\left[\dot{\Phi}^2 + \Phi'^2 + \frac{\lambda}{2}(\Phi^2 - 1)^2\right]. \tag{2.8}$$

From Figs. 2 and 4, we find some peaks in the energy density, by which we define the positions of moving walls ($y = \pm y_W(t)$). If a domain wall is symmetric, its position is defined by $\Phi(y) = 0$. However, in more general case, just as in the present case that the domain wall is oscillating around some moving point, it may be natural to define the position of a domain wall by the maximum point of its energy density.

In Figs. 2 and 4, we find the behavior of the collision as follows. Where the initial velocity $v = 0.4$, the collision occurs once, while it does twice where $v = 0.2$. To be

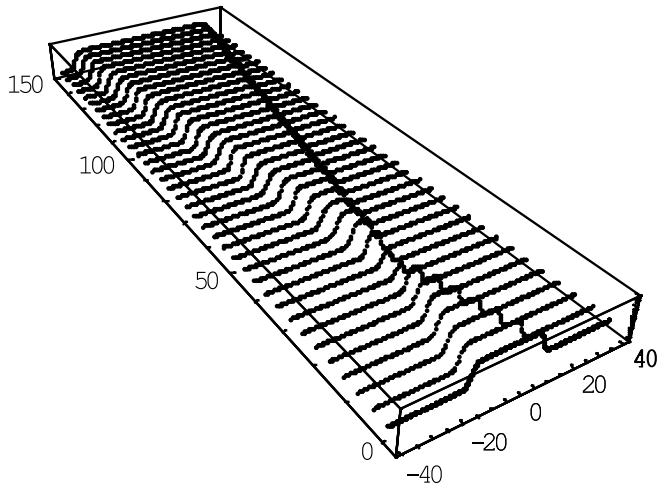

FIG. 1. Collision of two domain walls where the initial velocity $v = 0.4$. The time evolution of the scalar field Φ is shown from $t = 0$ to 150. The collision occurs once around $t = 31$. We set $\lambda = 1.0$.

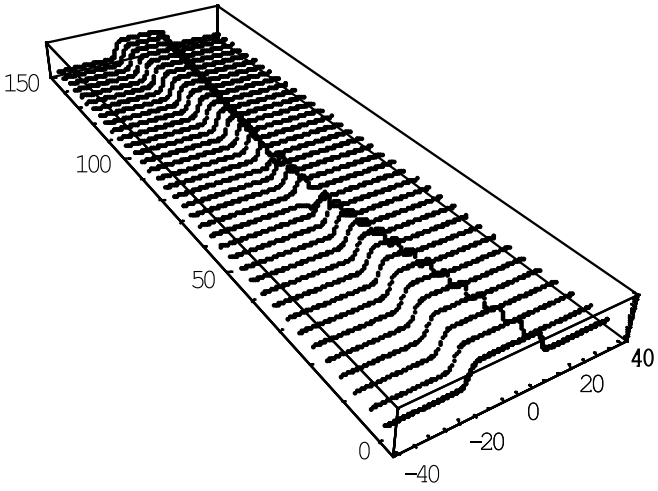

FIG. 3. Collision of two domain walls where the initial velocity $v = 0.2$. The time evolution of the scalar field Φ is shown from $t = 0$ to 150. We find that collision occurs twice, at $t \approx 58$ and 77. We set $\lambda = 1.0$.

precise, in the latter case, after two walls collide, they bounce, recede to a finite distance, and then return to collide again.

As shown by several authors [30–33], however, the result highly depends on the incident velocity v. In Appendix B, we show our analysis, which confirms the previous work. For a sufficiently large velocity, it is expected that a kink and an antikink will just bounce off once, because there is no time to exchange the energy during the collision process. In fact, it has been shown in [30] that two walls just bounce off once for $v \gtrsim 0.25$. For a lower velocity, we find multiple bounces when they collide. The number of bounces during the collision sensitively depends on the incident velocity. For example, the bounce occurs once for $v = 0.4$, while twice for $v = 0.2$. We also find many bounce solutions for other incident velocities, as shown in Appendix B (see also [30]). A set of the values of v which give the same number of bounce forms a fractal structure in the v-space as shown in Fig. 6 of [30]. If we change the incident velocity slightly, the number of bounces changes drastically.

III. PARTICLE PRODUCTION ON A MOVING DOMAIN WALL

A. Quantization of a particle on the domain wall and its production rate

Once we find the solution of colliding domain walls, we can evaluate the time evolution of a scalar field on the domain wall. Since we assume that we are living on one domain wall, we are interested in production of a particle confined to the domain wall. We assume that there is some

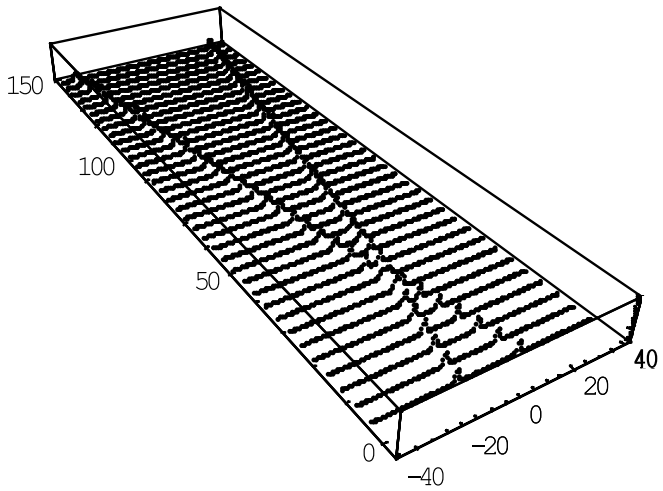

FIG. 2. The time evolution of scalar field energy density in the case of Fig. 1. The maximum point of ρ_Φ defines the position of a wall ($y = y_W(t)$).

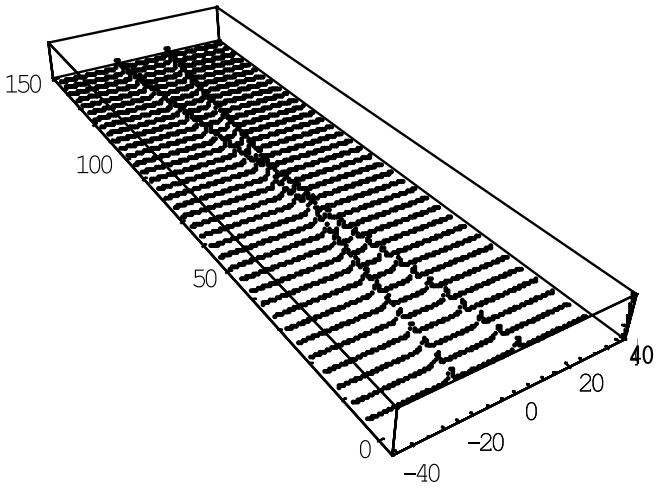

FIG. 4. The time evolution of scalar field energy density in the case of Fig. 3. From this figure, we find clearly that collision occurs twice.

coupling between a 5D scalar field Φ that is responsible for the domain wall and a particle on the domain wall. Because the value of the scalar field changes with time, we expect quantum particle production to occur. This may be important to a reheating mechanism for the colliding domain walls.

Hence we have to know the value of the scalar field Φ on the domain wall, i.e. $\Phi_{\rm W}(\tau) = \Phi[t, y_{\rm W}(t)]$. Since the wall is moving in a 5D Minkowski space, we have to use the proper time τ of the wall, which is given by

$$\tau = \int_0^t dt\sqrt{1 - \dot{y}_{\rm W}^2(t)}, \tag{3.1}$$

when we estimate the particle production in our 4-dimensional domain wall.

Let us consider a particle on the domain wall described by a scalar field ψ. Although the confined scalar field may also be extended in the 5th direction because the domain wall has a finite width, we assume here that this scalar field is 4-dimensional, which means that it has the value only at the position of the domain wall ($y = y_W(t)$). This ansatz may be justified as follows: Suppose that we have a 5D scalar field Ψ, which is confined on a wall with a width $d_\Psi(\sim d)$. Such a confined scalar field Ψ could be described as

$$\Psi = N\exp\left[-\frac{[y - y_W(\tau)]^2}{2d_\Psi^2}\right]\psi(x), \tag{3.2}$$

where N is a normalization constant. This assumption may be plausible because a width of the domain wall when two walls collide is the same as the original width d as seen from Fig. 5.

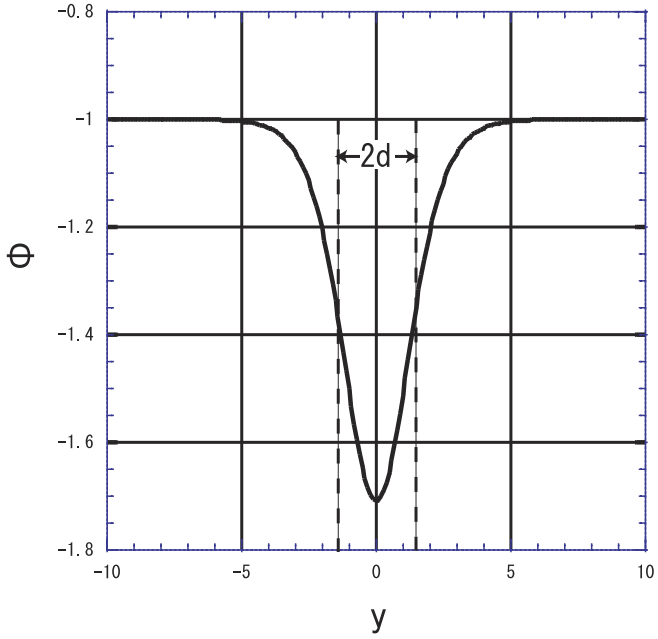

FIG. 5 (color online). The spatial distribution of the scalar field Φ when the domain walls collide. d is the thickness of the wall. The scalar field has a nonvanishing value for the effective width of $2d$ at the collision.

Assuming an interaction with the scalar field Φ as

$$\tfrac{1}{2}\bar{g}^2\Phi^2\Psi^2, \tag{3.3}$$

where $\bar{g}$ is a coupling constant, we find the dynamical equation for Ψ by

$$-\Box\Psi + \bar{g}^2\Phi^2\Psi = 0. \tag{3.4}$$

Inserting the ansatz (3.2), we obtain

$$Ne^{-\frac{[y-y_W(\tau)]^2}{2d_\Psi^2}}\left[\frac{\partial^2\psi}{\partial\tau^2} + (\bar{g}^2\Phi^2 - \nabla^2 + m_{\rm eff}^2)\psi\right] = 0, \tag{3.5}$$

where

$$m_{\rm eff}^2 = \frac{1 - \dot{y}_W^2}{d_\Psi^2}\left[1 - \frac{[y - y_W(\tau)]^2}{d_\Psi^2}\right] + \frac{(y - y_W)}{d_\Psi^2}\ddot{y}_W. \tag{3.6}$$

Equation (3.5) is nontrival only near the wall [$y \sim y_W(\tau)$] because of the gaussian distribution. Hence Φ in Eq. (3.5) should be evaluated on the wall [$y \sim y_W(\tau)$]. The effective mass term is estimated as $m_{\rm eff} \lesssim 1/d_\Psi$ because $|y - y_W(\tau)| \lesssim 1/d$, $\dot{y}_W^2 < 1$, and $|\ddot{y}_W| \lesssim \sigma|\dot{y}_W| < \sigma$, where $\sigma \sim \sqrt{\lambda} \sim 1/d$ is the oscillation frequency of the perturbations discussed given in Appendix C. The maximal value of acceleration of a domain wall ($\ddot{y}_W$) can be evaluated in the case of the oscillating field around a static wall.

Therefore, if we can ignore the mass term $m_{\rm eff}^2$ ($\lesssim 1/d_\Psi^2 \sim 1/d^2$), the equation for Ψ is approximated by the 4-dimensional equation for ψ as

$$\frac{\partial^2\psi}{\partial\tau^2} - \nabla^2\psi + \bar{g}^2\Phi_{\rm W}^2(\tau)\psi = 0, \tag{3.7}$$

where $\Phi_{\rm W}(\tau) = \Phi[y_W(\tau)]$. $\psi(x)$ is the 4-dimensional part of 5D scalar field Ψ. The assumption of dropping the mass term may be a good approximation in the present case because it turns out that the produced particles with the frequencies higher than $1/d$ is much less dominant as we will show later (see Sec. III B).

Once we find the basic equation for a scalar field ψ as Eq. (3.7), it is easy to quantize the scalar field ψ because our background spacetime is 4-dimensional Minkowski space. In a canonical quantization scheme [34], we expand ψ as

$$\psi(\tau, \boldsymbol{x}) = \sum_k [a_k\psi_k(\tau)u_k(\boldsymbol{x}) + a_k^\dagger\psi_k^*(\tau)u_k^*(\boldsymbol{x})], \tag{3.8}$$

where $u_k(\boldsymbol{x}) = (2\pi)^{-3/2}e^{i\boldsymbol{k}\cdot\boldsymbol{x}}$. The wave equation (3.7) for each mode is now

$$\ddot{\psi}_k + [k^2 + \bar{g}^2\Phi_{\rm W}^2(\tau)]\psi_k = 0, \tag{3.9}$$

where $k = |\boldsymbol{k}|$. Since the two domain walls are initially

far away from each other, the value of Φ_W is almost zero. We can quantize ψ by a usual quantization scheme. The eigen function with a positive frequency is given by

$$\psi_k^{(\mathrm{in})} = \frac{1}{\sqrt{2\omega_k}} e^{-i\omega_k \tau}, \tag{3.10}$$

where $\omega_k = \sqrt{k^2 + \bar{g}^2 \Phi_W^2(0)} \approx k$. We impose the equal time commutation relation for the operators a_k and $a_k^\dagger$

$$[a_k, a_{k'}] = 0, \tag{3.11}$$

$$[a_k^\dagger, a_{k'}^\dagger] = 0, \tag{3.12}$$

$$[a_k, a_{k'}^\dagger] = \delta_{kk'}, \tag{3.13}$$

where a_k and $a_k^\dagger$ are an annihilation and a creation operators. We then define a vacuum $|0\rangle_{\mathrm{in}}$ at $\tau = 0$ by a_k as

$$a_k |0\rangle_{\mathrm{in}} = 0, \quad \forall\ k. \tag{3.14}$$

After the collision of domain walls, we expect that the value of Φ_W again approaches zero (see the next subsection for details). We can also define the vacuum state $|0\rangle_{\mathrm{out}}$, which is different from the initial vacuum state $|0\rangle_{\mathrm{out}}$. The eigen function of ψ_k for $\tau \to \infty$ is then given by a linear combination of $\psi_k^{(\mathrm{in})}$ and $\psi_k^{(\mathrm{in})*}$ as

$$\psi_k^{(\mathrm{out})} = \alpha_k \psi_k^{(\mathrm{in})} + \beta_k \psi_k^{(\mathrm{in})*}, \tag{3.15}$$

and the annihilation and creation operators as

$$\bar{a}_k = \alpha_k a_k + \beta_k^* a_k^\dagger, \tag{3.16}$$

where α_k and β_k are the Bogolubov coefficients, which satisfy the normalization condition

$$|\alpha_k|^2 - |\beta_k|^2 = 1. \tag{3.17}$$

The Hamiltonian of this system is given by

$$:H: = -\int_{\tau=\mathrm{const}} :T_0^0: d^3\boldsymbol{x} = \sum_k a_k^\dagger a_k \omega_k, \tag{3.18}$$

where :: is the normal ordering operation. The creation of the particles with mode k is evaluated as

$$\langle 0|_{\mathrm{in}} :H_k: |0\rangle_{\mathrm{in}} = |\beta_k|^2 \omega_k \quad \text{as} \quad \tau \to \infty. \tag{3.19}$$

As a result, the number density and energy density of produced particles are given by

$$n = \int |\beta_k|^2 d^3\boldsymbol{k}, \tag{3.20}$$

$$\rho = \int |\beta_k|^2 \omega_k d^3\boldsymbol{k}. \tag{3.21}$$

B. Time evolution of a scalar field on the domain wall and particle production

Now we estimate the particle production by the domain-wall collision. In Figs. 6 and 7, we depict the time evolution of Φ_W on one moving wall with respect to τ. In Fig. 2, we found one collision point, which corresponds to a spike in Fig. 6, and the two-bounce in Fig. 4 gives two spikes in Fig. 7.

We also show the results for different values of the coupling constant λ in Figs. 8 and 9 ($\lambda = 10$). If Fig. 8 we find that when λ is larger than $\lambda = 10$, the spike of Φ_W becomes sharp. The same thing happens in the case of two bounces (see Fig. 9).

In Figs. 6–9, we find that Φ_W begins to oscillate after the collision. We also find that the period of these oscillations in Figs. 8 and 9 is shorter that those in Figs. 6 and 7. One may wonder whether this oscillation is realistic or not. This oscillation, however, turns out not to be a numerical error but a real oscillation of the domain wall. In Appendix C, using perturbation analysis we show there is one stable oscillation around the kink solution $\Phi_K(y)$. We expect that the oscillation is excited by the collision. In fact, the amplitude of the oscillation increases as the incident velocity v increases. At a large velocity limit ($v \gtrsim 0.6$), we find $\Phi_\infty^2 \approx 0.18(\gamma - 1)$, where Φ_∞ is the amplitude of the postoscillation.

Since the scalar field on the domain wall oscillates as $\Phi_W \approx \Phi_\infty \cos\sigma\tau$ after the collision, our wave Eq. (3.9) would be rewritten as

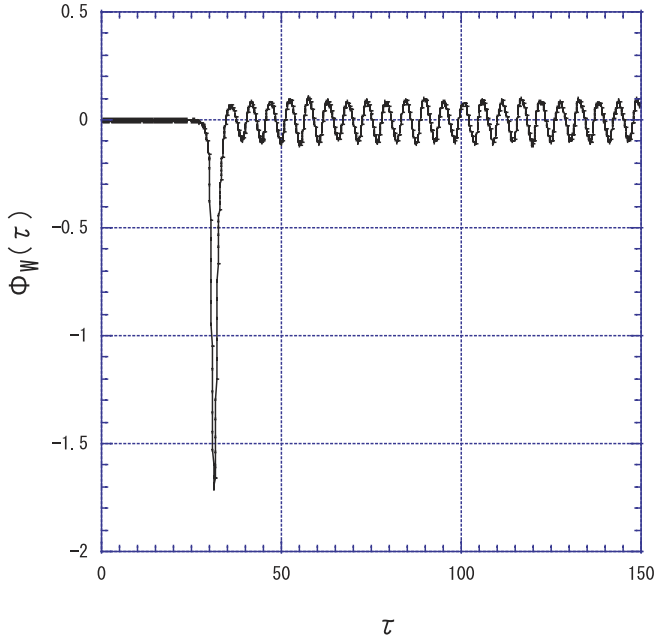

FIG. 6 (color online). Time evolution of a scalar field on one moving wall for $v = 0.4$, $\lambda = 1.0$. The value of the scalar field is given by $\Phi_W(\tau) = \Phi[t, y_W(t)]$, where $y_W(t)$ is the position of the wall and τ is the proper time on the wall.

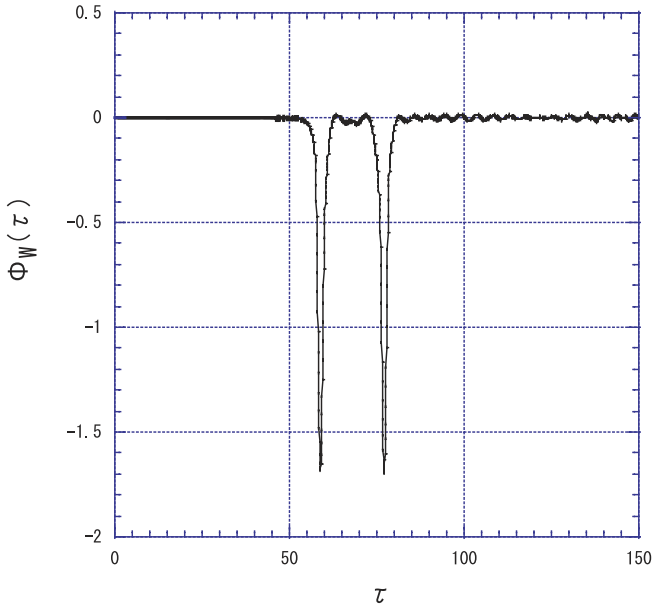

FIG. 7 (color online). Time evolution of a scalar field $\Phi_{\rm W}(\tau)$ on one moving wall for $v = 0.2$, $\lambda = 1.0$.

$$\ddot{\psi}_k + [k^2 + \tfrac{1}{2}\bar{g}^2\Phi_\infty^2(1 + \cos 2\sigma\tau)]\psi_k = 0, \qquad (3.22)$$

where $\sigma = \sqrt{3/2}\lambda^{1/2}$ is the eigenvalue of the perturbation eigen function, a so-called Methieu equation.

From this equation, we may wonder whether we can ignore this oscillation when we evaluate the particle production rate. In fact, we can discuss a preheating mechanism via a parametric resonance with a similar oscillating behavior [35], in conventional cosmology [1] as well as a brane world cosmology [36]. It is known that for a Methieu equation, there is an exponential instability $\psi_k \propto \exp(\mu_k t)$ within a set of resonance bands, where $\mu_k = \bar{g}\Phi_\infty^2/8$. This instability corresponds to an exponential growth of created particles, which is essential in the preheating mechanism. In order to get successful particle production by this resonance instability, however, we have to require a large value of $\bar{g}^2\Phi_\infty^2$. However, in the present simulation, it is rather small, e.g., $\Phi_\infty \sim 0.1$ where $v = 0.4$. Hence, we may ignore such particle production by parametric resonance in the present calculation. However, if the incident velocity is very fast, such as the speed of light, we may find a large oscillation. Then we could have an instant preheating process when domain walls collide. We also wonder whether or not the standard reheating mechanism due to the decay of an oscillating scalar field is effective. In this case, we have to evaluate the decay rate Γ_ϕ to other particles. Since $\Gamma_\phi \propto \bar{g}^4$, we expect that the reheating temperature is proportional to $\bar{g}^2$, which is small enough to be ignored. Note that there is another factor that reduces the decay rate where the potential is not a spontaneous symmetry breaking type [35].

In what follows, we ignore the creation due to the postoscillation stage. Hence, we just follow the procedure shown in the previous subsection. Using the evolution of the scalar field $\Phi_{\rm W}$, we calculate the Bogolubov coefficients α_k and β_k. In Table I, we show the results for three different parameters; v (the incident velocity), λ (the self-coupling constant of the scalar field), and $\bar{g}$ (the coupling constant to a particle ψ).

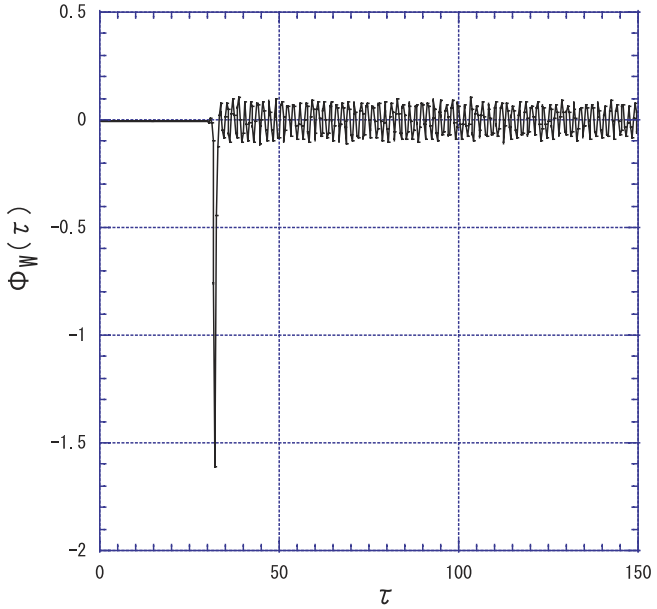

FIG. 8 (color online). Time evolution of a scalar field $\Phi_{\rm W}(\tau)$ on one moving wall for $v = 0.4$, $\lambda = 10$.

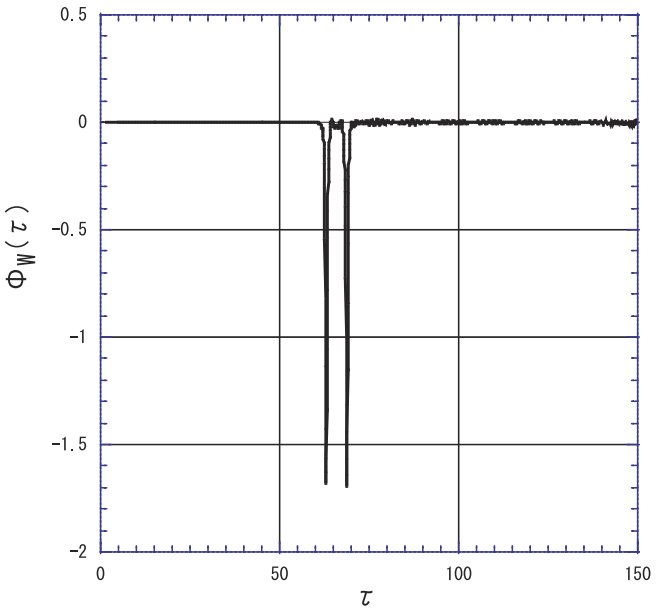

FIG. 9 (color online). Time evolution of a scalar field $\Phi_{\rm W}(\tau)$ on one moving wall for $v = 0.2$, $\lambda = 10$.

TABLE I. The number and energy densities (n and ρ) of created particles for the typical values of the coupling $\bar{g}$, the incident velocity v and the self-coupling λ. $d = \sqrt{2/\lambda}$ and N_b denote the width of the wall and the number of bounces at the collision, respectively.

$\bar{g}$	v	λ	d	N_b	n	ρ
0.01	0.4	1.0	1.414	1	3.69×10^{-7}	2.05×10^{-7}
		10	0.447		1.16×10^{-7}	2.05×10^{-7}
	0.2	1.0	1.414	2	7.19×10^{-7}	3.90×10^{-7}
		10	0.447		2.26×10^{-7}	3.91×10^{-7}
0.1	0.4	1.0	1.414	1	3.57×10^{-3}	2.01×10^{-3}
		10	0.447		1.16×10^{-3}	2.05×10^{-3}
	0.2	1.0	1.414	2	6.65×10^{-3}	3.81×10^{-3}
		10	0.447		2.24×10^{-3}	3.88×10^{-3}

From Table I, we find the following three features: (1) The produced energy density ρ depends very much on $\bar{g}$. We study two cases with $\bar{g} = 0.01$ and 0.1. The energy density for $\bar{g} = 0.1$ is 10^4 times larger than that for $\bar{g} = 0.1$, which means that ρ is proportional to $\bar{g}^4$. (2) The energy density ρ for $v = 0.2$ is twice larger than that for $v = 0.4$. It may be so because the bounce occurs twice for $v = 0.2$, while once for $v = 0.4$. (3) The energy density is less sensitive to λ.

We also investigate several different initial velocities because the collisional process is very sensitive to its incident velocity. We analyze many cases with two bounces, with three bounces, with four bounces, etc., in the range $v = 0.2 - 0.25$, as shown in Appendix B. Using those numerical data, we also evaluate the number and energy densities of the particles created at the collision. The results are summarized in Table II.

From Table II, we confirm the above three features (1)–(3). In particular, it becomes more clear that the energy density is proportional to the number of bounces N_b.

We can summarize our results by the following empirical formula

$$n \approx 25 d \bar{g}^4 N_b, \tag{3.23}$$

$$\rho \approx 20 \bar{g}^4 N_b. \tag{3.24}$$

If the energy of the particles is thermalized by interaction and a thermal equilibrium state is realized, we can estimate the reheating temperature by

$$\rho = \frac{\pi^2}{30} g_{\rm eff} T_{\rm R}^4, \tag{3.25}$$

where $g_{\rm eff}$ is the effective number of degrees of freedom of particles. Hence we find the reheating temperature by the domain-wall collision as

$$T_{\rm R} = \left(\frac{\pi^2}{30}\right)^{-1/4} g_{\rm eff}^{-1/4} \rho^{1/4} \approx 0.88 \times \left(\frac{g_{\rm eff}}{100}\right)^{-1/4} \bar{g} N_b^{1/4}. \tag{3.26}$$

In order to see more details, in Figs. 10 and 11, we show a spectrum of the produced particles of number density n, i.e.,

$$n = \int_0^\infty dk n_k \quad \text{with} \quad n_k = 4\pi |\beta_k|^2 k^2. \tag{3.27}$$

The spectrum n_k is well fitted as a Gaussian distribution as

$$n_k \approx 4\pi A e^{-\frac{k^2}{2k_0^2}}, \tag{3.28}$$

TABLE II. The number and energy densities (n and ρ) of created particles with respect to the number of bounces N_b. v and d are the incident velocity and the width of the wall, respectively. We set $\bar{g} = 0.01$.

N_b	v	λ	d	n	ρ
2	0.225	1.0	1.414	7.03×10^{-7}	3.72×10^{-7}
		10	0.447	2.21×10^{-7}	3.71×10^{-7}
	0.238	1.0	1.414	7.08×10^{-7}	3.78×10^{-7}
		10	0.447	2.23×10^{-7}	3.78×10^{-7}
3	0.2062	1.0	1.414	1.10×10^{-6}	6.07×10^{-7}
		10	0.447	3.45×10^{-7}	6.06×10^{-7}
	0.2049	1.0	1.414	1.09×10^{-6}	6.01×10^{-7}
		10	0.447	3.43×10^{-7}	6.01×10^{-7}
	0.2298	1.0	1.414	1.10×10^{-6}	6.04×10^{-7}
		10	0.447	3.43×10^{-7}	6.02×10^{-7}
	0.22933	1.0	1.414	1.09×10^{-6}	6.03×10^{-7}
		10	0.447	3.44×10^{-7}	6.01×10^{-7}
4	0.229283	1.0	1.414	1.47×10^{-6}	8.10×10^{-7}
		10	0.447	4.61×10^{-7}	8.09×10^{-7}
	0.2292928	1.0	1.414	1.47×10^{-6}	8.16×10^{-7}
		10	0.447	4.62×10^{-7}	8.17×10^{-7}

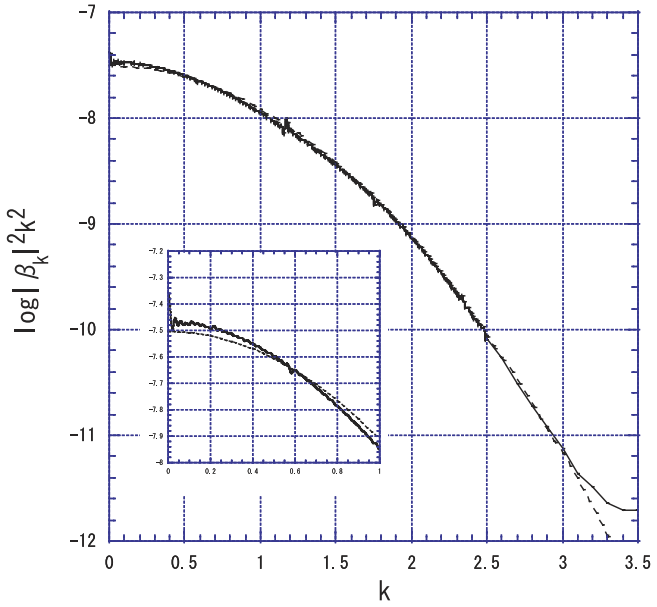

FIG. 10 (color online). Spectrum of the particles created at the collision. We plot $\log|\beta_k|^2k^2$ with respect to k for $v = 0.4$, $\lambda = 1.0$, $\bar{g} = 10^{-2}$. The Gaussian distribution is plotted by a dotted line, which gives a good approximation for $k \leq 3$. In the small box, we enlarge the low frequency region ($k \leq 1$) to see the deviation from the Gaussian distribution.

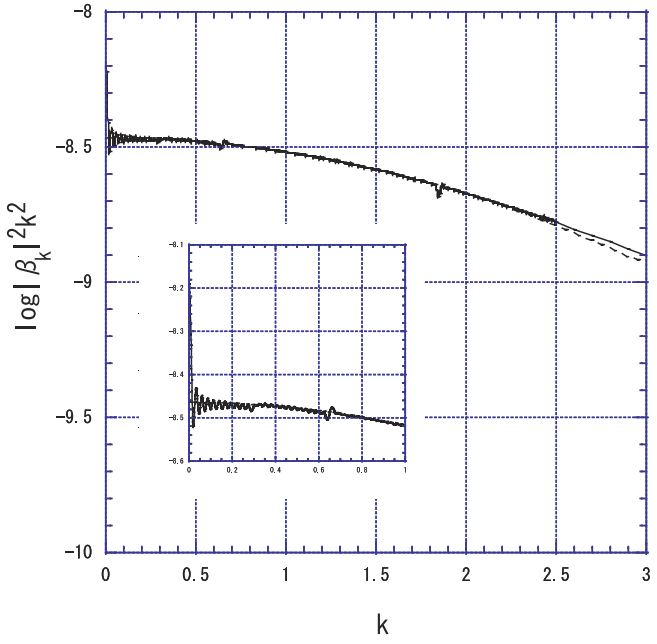

FIG. 11 (color online). Spectrum of the particles created at the collision. We plot $\log|\beta_k|^2k^2$ with respect to k for $v = 0.4$, $\lambda = 10$, $\bar{g} = 10^{-2}$. The Gaussian distribution is plotted by a dotted line, which gives a good approximation for $k \leq 2.5$. In the small box, we enlarge the low frequency region ($k \leq 1$) to see the deviation from the Gaussian distribution.

where $k_0 = 0.73$ and $A = 3.12 \times 10^{-8}$ for Fig. 10 and $k_0 = 2.04$ and $A = 3.43 \times 10^{-9}$ for Fig. 11, although there is small deviation partially. These parameters can be described by physical quantities as $k_0 \approx 1/d$ and $A \approx \Phi_0 d^2 \bar{g}^4$. The reason is well understood. $k_0 \approx 1/d$ means that the typical wave number is given by the width of the scalar field when domain walls collide (see Fig. 5). As for β, it corresponds to the "reflection" coefficient of the "potential" given in Figs. 6–9. It will be proportional to the coupling constant $\bar{g}^2$, and the reflection rate ($|\beta|^2$) will be related to the potential depth Φ_0 and the square of the width d^2. This result may support our ansatz that a scalar field ψ is 4-dimensional because the particles with the frequencies higher than $1/d$ are produced very little. The effect of finite width of the walls on particle production may not be important.

Integrating the fitting spectrum (3.28), we obtain

$$n = \int_0^\infty n_k dk = (2\pi)^{3/2} \Phi_0 d \bar{g}^4 \approx 25 d \bar{g}^4, \tag{3.29}$$

$$\rho = \int_0^\infty n_k \omega_k dk = 4\pi \Phi_0 \bar{g}^4 \approx 20 \bar{g}^4, \tag{3.30}$$

whose values are exactly the same as those obtained by numerical integration in the case with one bounce [see Eqs. (3.23) and (3.24)]. We expect that they are enhanced by the factor N_b when we find N_b bounces at the collision.

Therefore, although we obtain particle creation numerically, the result is easily understood and summarized by a simple formula.

IV. SUMMARY AND DISCUSSION

We have studied particle production at the collision of two domain walls in 5D Minkowski spacetime. This may provide the reheating mechanism of an ekpyrotic (or cyclic) brane universe, in which two BPS branes collide and evolve into a hot big bang universe. We evaluated the production rate for particles confined to the domain wall. The energy density of created particles was approximated as $\rho \approx 4\pi \Phi_0 \bar{g}^4 N_b$ where Φ_0 is the maximum amplitude of Φ_W, N_b is the number of bounces at the collision, and $\bar{g}$ is a coupling constant of a particle to the scalar field of a domain wall. If this energy is converted into standard matter fields, we find the reheating temperature as $T_R \approx 0.88 \times \bar{g} N_b^{1/4} (g_{\rm eff}/100)^{-1/4}$. We find that the particle creation is affected more greatly by the coupling constant $\bar{g}$ than the other two parameters v and λ. The initial velocity changes the collision process, that is, the number of bounces at the collision, but this is less sensitive to the temperature. The thickness of a domain wall d (or a self-coupling constant λ) changes the width of potential $\Phi_w^2(\tau)$ of a particle field (ψ), and it changes the typical energy scale of created particles, which is estimated as $\omega \sim 1/d$.

In order to produce a successful reheating, a reheating temperature must be higher than 10^2 GeV, because we wish to explain the baryon number generation at the electro-weak energy scale [2]. Since Eq. (3.26) is written in the following form;

$$m_\eta \approx 1.1 N_b^{-1/4} \bar{g}^{-1} T_{\rm R} \approx 1.1 \times 10^7 [\mathrm{GeV}] N_b^{-1/4} \left(\frac{\bar{g}}{10^{-5}}\right)^{-1} \left(\frac{T_{\rm R}}{10^2\ \mathrm{GeV}}\right), \quad (4.1)$$

we find a constraint on the fundamental energy scale m_η as $m_\eta \gtrsim 1.1 \times 10^7$ GeV for $\bar{g} = 10^{-5}$ and $m_\eta \gtrsim 1.1 \times 10^4$ GeV for $\bar{g} = 10^{-2}$, which are slightly larger than TeV scale. Here we assume $g_{\rm eff} = 100$.

In the present work, we considered 3-dimensional domain walls in 5-dimensional Minkowski space and showed that particle production at the two-wall collision may provide a successful mechanism for reheating in the ekpyrotic universe. In string/M theory, however, we expect higher dimensions, e.g., 10 or 11. If we compactify it to the effective 5-dimensional spacetime, our work can be applicable to such a mode. Moreover, if we discuss a collision of p-dimensional walls (branes) in $(p+2)$-dimensional spacetime, our approach can also be extended.

In this paper, we have not taken account of effects from background spacetime. We are planning to study how such a generalization affects the present results about particle creation at the collision.

ACKNOWLEDGMENTS

We would like to thank S. Mizuno, T. Torii, and D. Wands for useful discussions. This work was partially supported by the Grant-in-Aid for Scientific Research Fund of the MEXT (Grant No. 14540281) and by the Waseda University Grant for Special Research Projects and for The 21st Century COE Program (Holistic Research and Education Center for Physics Self-organization Systems) at Waseda University.

APPENDIX A: NUMERICAL METHOD

For our numerical analysis of the domain-wall collision, we solve the partial differential Eq. (2.3) on discrete spatial grids with a periodic boundary condition. The scalar field on the grid points is defined by $\Phi_n(t) = \Phi(y_n, t)$, where $y_n = n \triangle y$, for $n = 1, 2, \ldots, N$. We use the fourth-order center difference scheme to approximate the second spatial derivative [37] as

$$\frac{\partial^2 \Phi_n}{\partial y^2} = \frac{1}{12(\triangle y)^2}[-\Phi_{n-2} + 16\Phi_{n-1} - 30\Phi_n + 16\Phi_{n+1} - \Phi_{n+2}] + O[(\triangle y)^4]. \quad (A1)$$

This leads to a set of N coupled second-order ordinary differential equations (ODE's) for the Φ_n, i.e.,

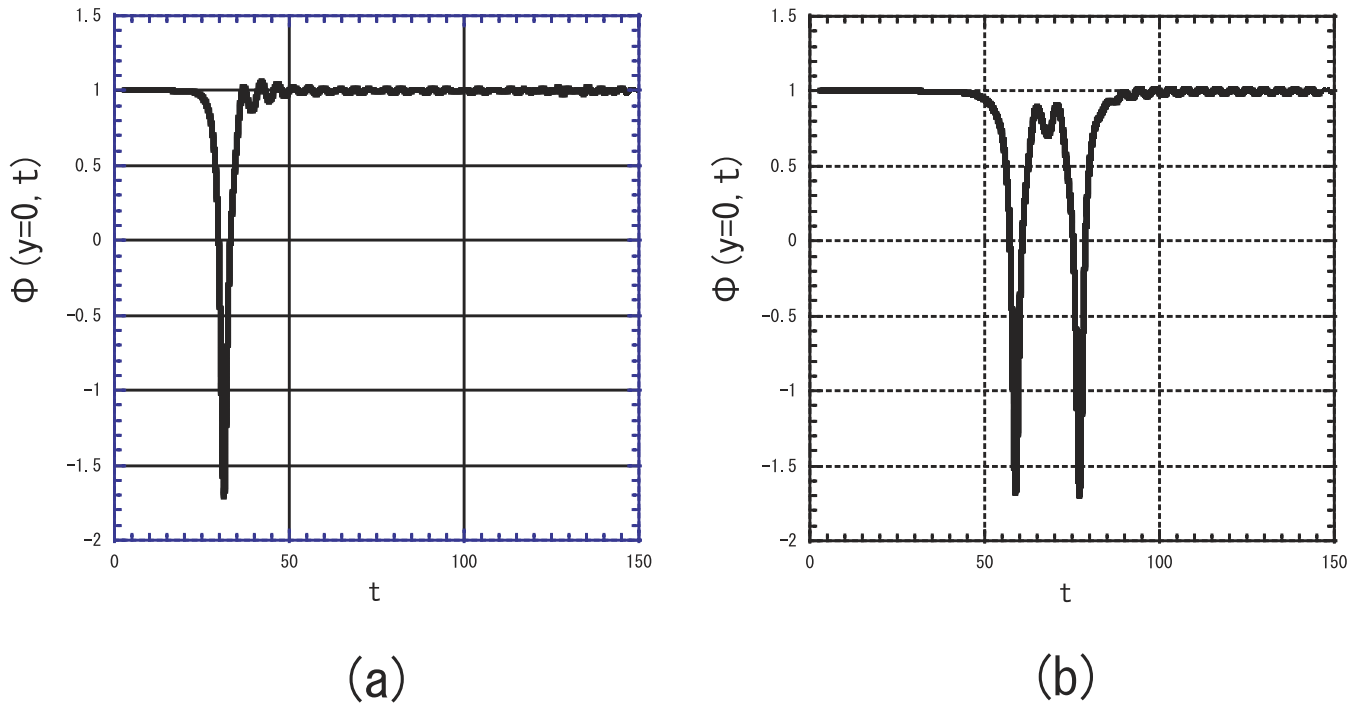

FIG. 12 (color online). Time evolution of Φ field at $y = 0$ are depicted for (a) $v = 0.4$ $\lambda = 1.0$ and (b) $v = 0.2$, $\lambda = 1.0$. The bounce occurs once for a large velocity (a), while two bounces are found for the slower velocity.

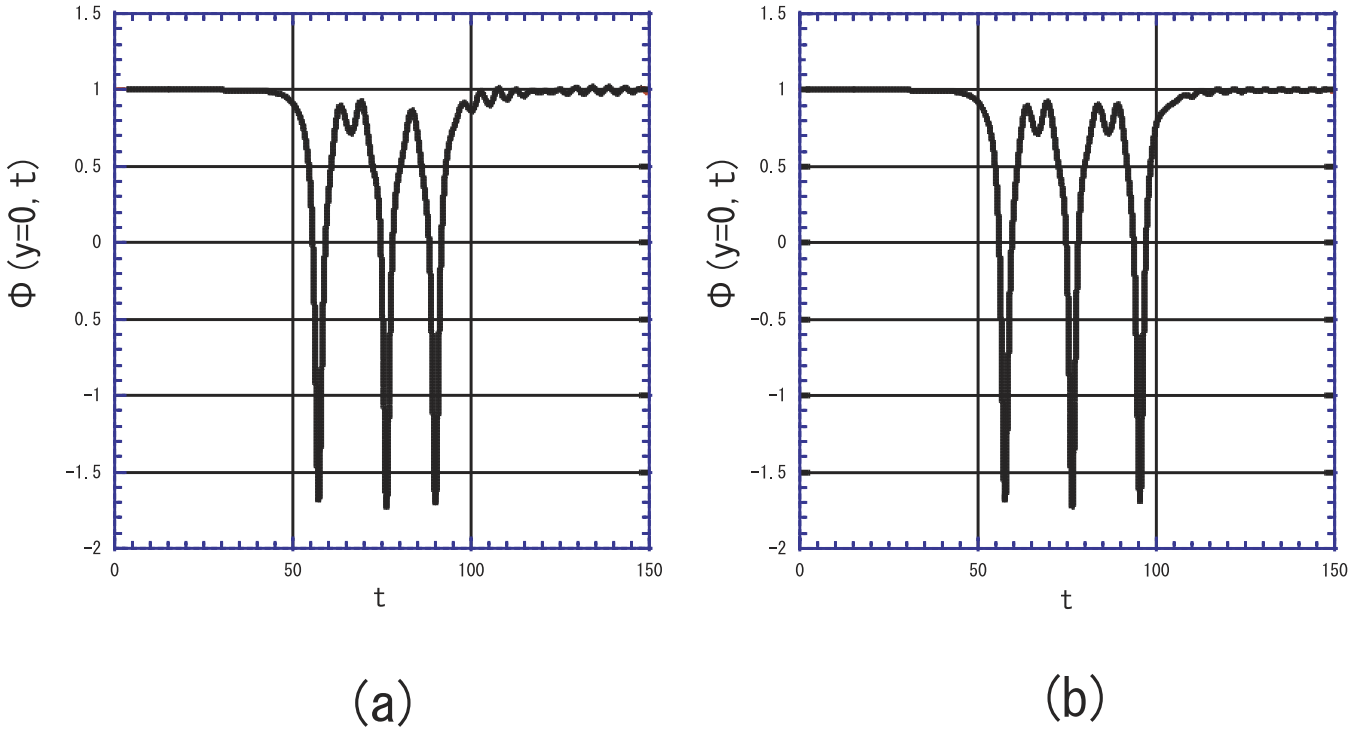

FIG. 13 (color online). Time evolution of Φ field at $y = 0$ are depicted for (a) $v = 0.2062$ $\lambda = 1.0$ and (b) $v = 0.2049$, $\lambda = 1.0$. Three bounces are found.

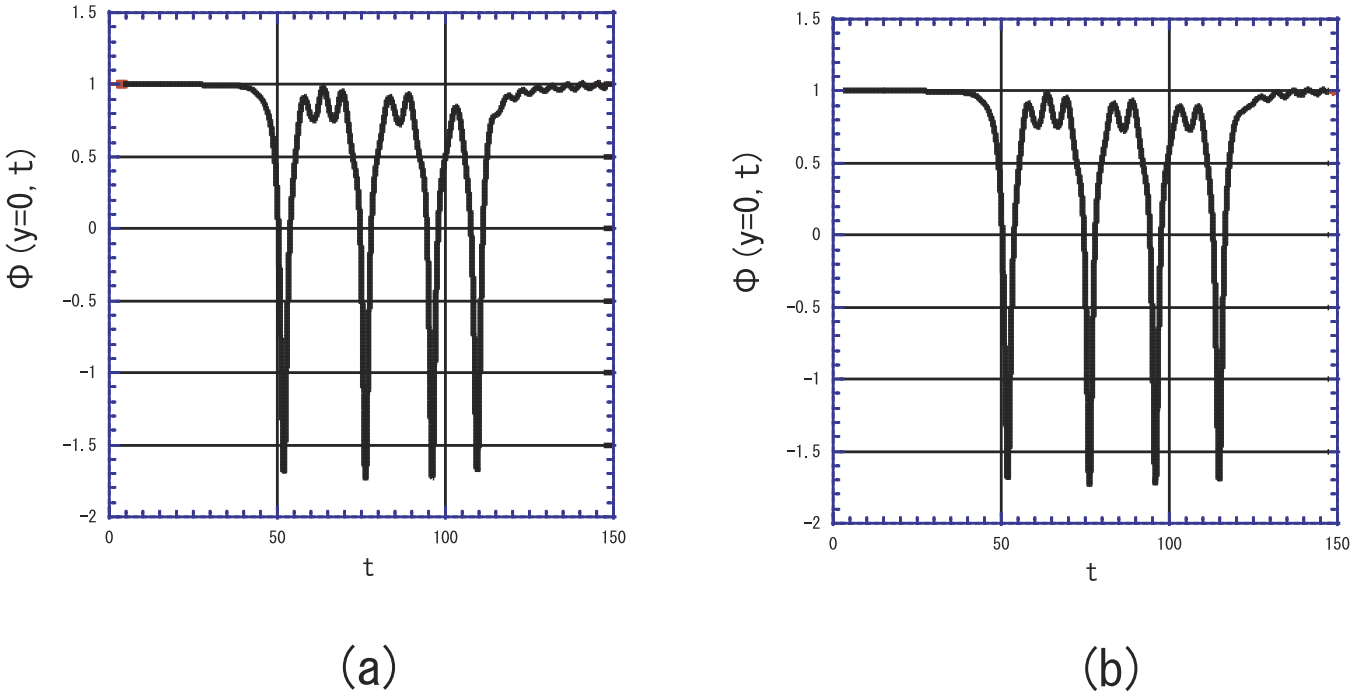

FIG. 14 (color online). Time evolution of Φ field at $y = 0$ are depicted for (a) $v = 0.229\,283$ $\lambda = 1.0$ and (b) $v = 0.229\,2928$, $\lambda = 1.0$. Four bounces are found.

$$\frac{d^2\Phi_n}{dt^2} = \frac{1}{12(\triangle y)^2}[-\Phi_{n-2} + 16\Phi_{n-1} - 30\Phi_n + 16\Phi_{n+1} - \Phi_{n+2}] - \lambda\Phi_n(\Phi_n^2 - 1). \quad \text{(A2)}$$

The ODE's (A2) are solved using a fourth-order Runge-Kutta scheme, and so our numerical algorithm is accurate to the fourth-order both in time and in space, with error of $O[(\triangle y)^4]$ and $O[(\triangle t)^4]$. For the boundaries, we set the left and right grid boundaries at $y_L = -40$ and $y_R = +40$, and impose the condition $\Phi(y = y_L, t) = \Phi(y = y_R, t) = -1$. The grid number is $N = 8000$ with a grid size of $\triangle y = 1.0 \times 10^{-2}$. The initial position of a wall y_0 is set by $y_0 = |y_L + (y_R - y_L + 1)/3| = 13$, equivalently, one-third of the numerical range. For time steps, we set $\triangle t = 0.7 \times \triangle y$.

As for the particle production process, we have to solve the second-order ordinary differential Eqs. (3.9) for each wave number k. By using the fourth-order Runge-Kutta scheme, we solve them for the wave number k of $0 < k < 100$ with the width $\triangle k = 1.0 \times 10^{-3}$. We estimate $|\beta_k|^2$ in the Eq. (3.15). Defining the functions this way:

$$W_1 \equiv \psi_k\dot{\psi}_k^* - \psi_k^*\dot{\psi}_k, \quad \text{(A3)}$$

$$W_2 \equiv \psi_k\dot{\psi}_k^* + \psi_k^*\dot{\psi}_k, \quad \text{(A4)}$$

$$W_3 \equiv \psi_k\psi_k^*, \quad \text{(A5)}$$

we use the formula

$$|\beta_k|^2 = \frac{(W_3 - W_1/2i\omega)^2 + (W_2/2\omega)^2}{4W_3}, \quad \text{(A6)}$$

to evaluate $|\beta_k|$.

APPENDIX B: NUMERICAL EXAMPLES OF SEVERAL BOUNCES AT THE COLLISION

We depict some numerical examples that show several bounces at the collision. First we show two typical examples in Fig. 12. The figures show the behaviors of the scalar field Φ at $y = 0$ with respect to t. Initially, when two domain walls are located at a large distance, the value of the scalar field at $y = 0$ is 1. Then the two walls approach and collide. At this point the value of $|\Phi - 1|$ increases. After the collision, it again decreases to the initial value. We find some small oscillation around the domain-wall structure excited by the collision.

From Fig. 12, we find there is one bounce for $v = 0.4$, while a bounce occurs twice for $v = 0.2$. In fact, the results are very much sensitive to the incident velocities as shown in [30].

Here we present several examples to show how the behaviors of the scalar field depend on v, which confirm the previous studies.

In Figs. 13(a), we show the case for $v = 0.2062$ and $v = 0.2049$, respectively. We find three bounces at the collision. Four-bounce solutions are depicted in Figs. 14(a) ($v = 0.229\,283$) and 14(b) ($v = 0.229\,2928$). These calculation shows that the detail collisional process is very sensitive to the incident velocity.

APPENDIX C: PERTURBATIONS OF A DOMAIN WALL

We show that the oscillation we find in Sec. III B is a proper oscillation around a static stable domain wall. To show it, we perturb the static domain-wall solution (2.4) as

$$\Phi = \Phi_K(y) + \delta\Phi(t, y). \quad \text{(C1)}$$

In this appendix, we use the dimensionless variables rescaled by η. Substituting this into Eq. (2.3) and linearizing it, we obtain

$$\delta\ddot{\Phi} - \delta\Phi'' + \lambda(3\Phi_K^2 - 1)\delta\Phi = 0. \quad \text{(C2)}$$

Setting

$$\delta\Phi = e^{-i\sigma t}F(y), \quad \text{(C3)}$$

and introducing new variable $\bar{y} = \tanh(y/d)$, we rewrite Eq. (C2) as

$$(1 - \bar{y}^2)\frac{d^2F}{d\bar{y}^2} - 2\bar{y}\frac{dF}{d\bar{y}} + 2\left[3 - \frac{2 - \sigma^2/\lambda}{1 - \bar{y}^2}\right]F = 0. \quad \text{(C4)}$$

The solution is given by the associated Legendre function. Imposing the boundary condition ($F \to 0$ as $y \to \infty$), we have two regular solutions; $F(\bar{y}) = P_2^2(\bar{y})$ with $\sigma = 0$ and $P_2^1(\bar{y})$ with $\sigma = \sqrt{3/2}\lambda^{1/2}$.

The solution of the former mode is just corresponds to a boost of a kink solution in the y direction, because we find $F(y) \approx \Phi_K(y) - \Phi_K(y - dy)$. The solution of the latter is the oscillation mode we find in Sec. II B. In fact, taking the average over ten cycles in the oscillation after the collision in Fig. 6, we obtain a mean angular frequency of about 1.17, which is very close to $\sigma = \sqrt{3/2} \sim 1.22$. The ratio is about 0.96. We also evaluate the angular frequency for other cases. We find $1.33 = 1.09\sigma$ for Fig. 7, $3.67 = 0.95\sigma$ for Fig. 8, and $4.18 = 1.08\sigma$ for Fig. 9. From the figures, we also find that the amplitude of oscillation gets larger as the incident velocity is faster. This is because the excitation energy of a wall at the collision will be large for a large velocity.

We then conclude that the oscillations after the collision of two domain walls are the proper oscillations around a stable domain wall.

[1] A. Linde, *Particle Physics and Inflationary Cosmology* (Harwood, Academic, Chur, Switzerland, 1990).
[2] E.W. Kolb and M. S. Turner, *The Early Universe* (Westview Press, Boulder, Colorado, 1990).
[3] K. Akama, Lect. Notes Phys. **176**, 267 (1982); V. A. Rubakov and M. E. Shaposhnikov, Phys. Lett. B **125**, 136 (1983); M. Visser*ibid.***159**, 22 (1985).
[4] I. Antoniadis, Phys. Lett. B **246**, 377 (1990); N. Arkani-Hamed, S. Dimopoulos, and G. Dvali*ibid.***429**, 263 (1998); **436**, 257 (1998).
[5] P. Hořava and E. Witten, Nucl. Phys. **B460**, 506 (1996); **B475**, 94 (1996).
[6] J. Polchinski, *String Theory I & II* (Cambridge University Press, Cambridge, 1998).
[7] J. Polchinski, Phys. Rev. Lett. **75**, 4724 (1995).
[8] L. Randall and R. Sundrum, Phys. Rev. Lett. **83**, 4690 (1999).
[9] P. Binétruy, C. Deffayet, and D. Langlois, Nucl. Phys. **B565**, 269 (2000); P. Binétruy, C. Deffayet, U. Ellwanger, and D. Langlois, Phys. Lett. B **477**, 285 (2000).
[10] C. Csaki, M. Graesser, C. Kolda, and J. Terning, Phys. Lett. B **462**, 34 (1999); N. Kaloper, Phys. Rev. D **60**, 123506 (1999); T. Nihei, Phys. Lett. B **465**, 81 (1999); H. S. Reall*ibid.***465**, 103506 (1999).
[11] A. Lukas, B. A. Ovrut, K. S. Stelle, and D. Waldram, Phys. Rev. D **59**, 086001 (1999); A. Lukas, B. A. Ovrut, and D. Waldram*ibid.***60**, 086001 (1999).
[12] K. Maeda, Prog. Theor. Phys. Suppl. **148**, 59 (2003); K. Maeda, Lect. Notes Phys. **646**, 323 (2004).
[13] R. Maartens, gr-qc/0101059; Prog. Theor. Phys. Suppl. **148**, 213 (2003); gr-qc/0312059.
[14] D. Langlois, gr-qc/0207047; Prog. Theor. Phys. Suppl. **148**, 181 (2003).
[15] P. Brax and C. van de Bruck, Classical Quantum Gravity **20**, 201R (2003); P. Brax, C. van de Bruck, and A. C. Davis, hep-th/0404011.
[16] M. Sasaki, T. Shiromizu, and K. Maeda, Phys. Rev. D **62**, 024008 (2000); S. Mukohyama, T. Shiromizu, and K. Maeda*ibid.***62**, 024028 (2000).
[17] K. Maeda and D. Wands, Phys. Rev. D **62**, 124009 (2000).
[18] J. Khoury, B. A. Ovrut, P. J. Steinhardt, and N. Turok, Phys. Rev. D **64**, 123522 (2001); J. Khoury, B. A. Ovrut, N. Seiberg, P. J. Steinhardt, and N. Turok*ibid.***65**, 086007 (2002); **66**, 046005 (2002); A. J. Tolley and N. Turok*ibid.***66**, 106005 (2002).
[19] P. J. Steinhardt and N. Turok, Phys. Rev. D **65**, 126003 (2002); J. Khoury, P. J. Steinhardt, and N. Turok, Phys. Rev. Lett. **92**, 031302 (2004).
[20] D. H. Lyth, Phys. Lett. B **524**, 1 (2002).
[21] R. Brandenberger and F. Finelli, J. High Energy Phys. **11**, 056 (2001); F. Finelli and R. Brandenberger, Phys. Rev. D **65**, 103522 (2002).
[22] J. Martin, P. Peter, N. Pinto Neto, and D. J. Schwarz, Phys. Rev. D **65**, 123513 (2002); P. Peter and N. Pinto-Neto*ibid.* **66**, 063509 (2002); J. Martin, P. Peter, N. Pinto-Neto, and D. J. Schwarz*ibid.***67**, 028301 (2003).
[23] S. Tsujikawa, Phys. Lett. B **526**, 179 (2002); S. Tsujikawa, R. Brandenberger, and F. Finelli, Phys. Rev. D **66**, 083513 (2002); L. E. Allen and D. Wands, Phys. Rev. D **70**, 063515 (2004).
[24] J. M. Cline, H. Firouzjahi, and P. Martineau, J. High Energy Phys. 11 (2002) 041; N. Barnaby and J. M. Cline, Phys. Rev. D **70**, 023506 (2004).
[25] J. Martin, G. N. Felder, A.V. Frolov, M. Peloso, and L. Kofman, Phys. Rev. D **69**, 084017 (2004); J. Martin, G. N. Felder, A.V. Frolov, L. Kofman, and M. Peloso, hep-ph/0404141.
[26] G. Dvali and A. Vilenkin, Phys. Rev. D **67**, 046002 (2003).
[27] N. D. Antunes, E. J. Copeland, M. Hindmarsh, and A. Lukas, Phys. Rev. D **68**, 066005 (2003); N. D. Antunes, E. J. Copeland, M. Hindmarsh, and A. Lukas*ibid.***69**, 065016 (2004).
[28] M. Eto and N. Sakai, Phys. Rev. D **68**, 125001 (2003); M. Eto, S. Fujita, M. Naganuma, and N. Sakai*ibid.***69**, 025007 (2004).
[29] L. Windrow, Phys. Rev. D **40**, 1002 (1989).
[30] P. Anninos, S. Oliveira, and R. A. Matzner, Phys. Rev. D **44**, 1147 (1991).
[31] V. Silveira, Phys. Rev. D **38**, 3823 (1988).
[32] T. I. Belova and A. E. Kudryavtsev, Physica D (Amsterdam) **32**, 18 (1988).
[33] D. K. Campbell, J. F. Schonfeld, and C. A. Wingate, Physica D (Amsterdam) **9**, 1 (1983).
[34] N. D. Birrell and P. C.W. Davies, *Quantum Fields In Curved Space* (Cambridge University Press, Cambridge, England, 1982).
[35] L. Kofman, A. D. Linde, and A. A. Starobinsky, Phys. Rev. Lett. **73**, 3195 (1994); L. Kofman, A. D. Linde, and A. A. Starobinsky, Phys. Rev. D **56**, 3258 (1997).
[36] S. Tsujikawa, K. Maeda, and S. Mizuno, Phys. Rev. D **63**, 123511 (2001).
[37] R.W. Hornbeck, *Numerical Methods* (Prentice-Hall, NJ, 1975).